Numerical study on aerosol sampling in a nuclear facility duct with a 90-degree elbow

K. Han, PhD, PE
Member

ABSTRACT

Due to the challenging design requirements, elbows are often unavoidable in duct configuration, and these 90-degree bends introduce swirl, velocity variations, recirculation, and secondary flow. These disturbances make it difficult for nuclear facilities to meet particle sampling standards. A series of numerical analyses are conducted to track aerosols in a nuclear facility duct having a 90-degree elbow with the assistance of computational fluid dynamics (CFD). A turbulence model, a continuity, and a momentum, a discrete phase model, and species transport equations are solved simultaneously to track aerosols in the duct. The effect of turbulence models, turbulent dispersion models, droplet drag model, aerosol amount, aerosol spray configuration, guide vanes, and mixers are investigated. Simulation results are analyzed per relevant testing codes such as DOE-HDBK-1169, ASME AG1, ISO 14644-3, ACGIH, and ANSI/HPS N13.1.

INTRODUCTION

Deep bed sand (DBS) filters are a potential alternative to HEPA (High Efficiency Particulate Air) filter, especially for large capacity nuclear facilities that require long term mission and fire/explosion resistant. A typical DBS filter has a graded layer of rock, gravel, and sand several feet thick. The airflow direction is upward, so particle size decreases in the direction of flow. Air-aerosol mixing test and leak test procedures for DBS filters are outlined in ASME AG-1-2019. Dioctyl Phthalate (DOP) aerosols less than 0.0001" (3 μm) diameter are preferred for these tests. The aerosol concentrations over the entire sampling plane should not exceed ±20% of the average concentration as specified in ASME AG-1 (2019). This requirement is challenging for ducts with flow disturbance such as 90-dgree elbows, branch entry, etc., which are often unavoidable in duct configurations. A flow mixer may be considered to meet this concentration distribution. Downstream aerosol sampling probes should be positioned as established in ACGIH Industrial ventilation code (1998). For square or rectangular ducts, the cross-section should be divided into several equal rectangular sections, with a maximum center-to-center distance not exceeding 6" (0.15 m). Given the typical duct sizes of DBS filters, this distance requirement is difficult to meet. DBS filters can be as large as a football field, and connecting duct diameters can easily exceed 10' (3 m) due to the large flow rate and flow speed requirements. This large duct size presents many challenges. The number of sampling points can exceed several hundred. Given the runtime of the aerosol generator or the expected long test times, many samplers may be required. It can also be difficult to prepare sampling ports in concrete ducts and locate sampling plane. Other standards, such as ANSI/HPS N13.1 and 40 CFR 60 Method 1, can be considered to reduce the number of sampling points. However, these standards require verficiation of swirl flow. Complex flow patterns are inevitable in ducts with turns, branches, cross-sectional changes, and entries. This swirl free condition requires flow straighteners, which increase pressure losses.

K. Han is a Sr. fellow engineer at Savannah River Nuclear Solutions.

This increases the size of the fan/motor and makes inspection/cleaning difficult.

These challenging situations require intensive engineering studies, and computational fluid dynamics (CFD) studies can help in selecting the right location of the sampling plane and determining the duct layout. It can also be used to select the aerosol spray location and appropriate flow devices such as mixers, guidevanes, and flow straighteners. However, CFD should be used with caution considering the sensitivity of turbulence model, turbulent dispersion model setting, and droplet drag model are considered. In this study, the above-mentioned parameters are investigated with the help of commercial CFD package, especially for a duct having 90-degree eblow.

NUMERICAL METHOD

For aerosol tracking, species transport equations along with a turbulence model, a discrete phase model, a continuity equation, and a momentum equation are solved simultaneously. An arbitrary square duct with a width and height of 10' (D, 3 m) is constructed, and a sharp 90-degree turn is placed in the middle of the duct as shown in fig. 1. The duct lengths before and after the 90-degree turn are 100' (30 m) each. One end of the duct is assigned as the inlet velocity boundary, and the other end is designated as the pressure outlet boundary. A predetermined velocity profile is introduced to the inlet boundary to investigate the effect of duct geometry changes.

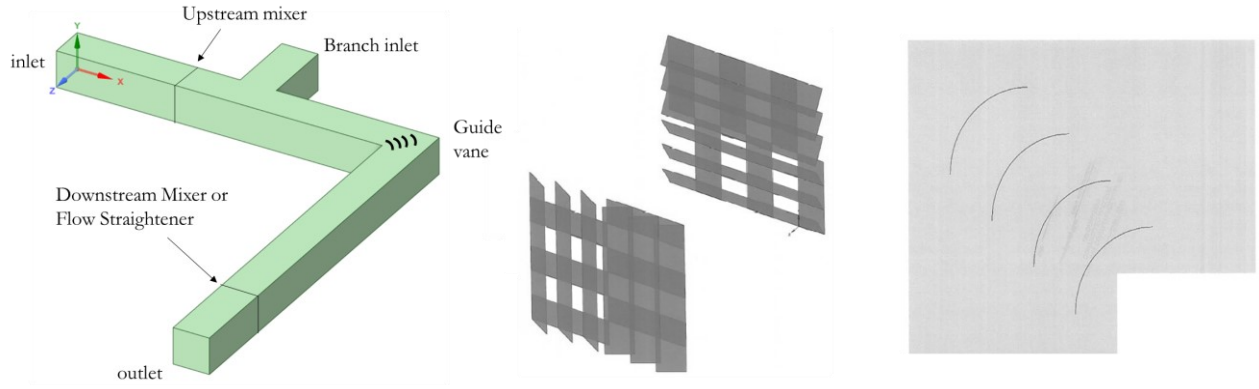

Figure 1 (a) Numerical domain, (b) Louver-baffle mixer, and (c) Guide vanes.

The aerosol spray locations are varied, and DOP is used as the aerosol. DOP is an oily liquid that does not evaporate readily. Hence, evaporation of DOP is neglected, and it is assumed that the impinging droplets spread or stick to the wall. The density of DOP is very close to that of water (PubChem, 2024). The effect of DOP particle size (d), aerosol sparay velocity (v_d), number of nozzles (n), and nozzle cone angle (α) are investigated. The aerosol amount (m) is 10 μg/l per ISO 14644-3 (2019). The average air speed in the duct is 2500 fpm (12.7 m/s) as specified in DOE-HDBK-1169 (2022). The velocity profile (vf) is varied while maintaining the total inlet air flow rate to determine the aerosol concentration distribution. The uniform velocity profile (U) is used as the default, while fully developed (F) and two triangle (T) velocity profiles are also investigated. Four different turbulence models (TM) including the standard k-ε model (S), the Re-Normalization Group k-ε model (RNG), the Realizable k-ε turbulence model (R), and the Reynolds Stress Model (RSM) are tested with scalable wall functions to avoid the deterioration of standard wall functions under grid refinement below the critical distance from the wall. The fluid phase is treated as a continuum by solving the Navier-Stokes equations, while the dispersed phase is solved by tracking liquid droplet particles through the calculated flow field. Considering the lower volume fraction of the dispersed second phase,

particle-particle interactions are neglected. Particle dispersion by turbulent fluctuations is modeled with the discrete random walk (DRW) model (Gosman and Loannides, 1983). Mixing and transport of species (dry air and aerosol) are modeled by solving conservation equations describing convection and diffusion for each consitituent species. Drag is one of the key factors in the force balance that determines the trajectories of discrete phase particles in turbulent flows. Spherical (SP) drag law (Morsi and Alexander, 1972), non-spherical (NSP) drag law (Haider and Levenspiel, 1989), and Stokes-Cunningham (SC) drag law (Ounis et al., 1991) are compared. The flow straightener (ST) is modeled using a porous media to depict AMCA type (ASME MFC-3M-2004, 2005) for case 25. The length of the flow straightener is 0.45D and the loss coefficient is 0.25. The effects of louver-baffle mixing device (M) and guid vanes (G) are also investigated. Two louvered strip mixers are arranged in series for case 26 and 29. The second mixer is rotated 90° with respect to the first mixer. The distance between the mixers is 1.5D (Faison et al. 1970). The downstream mixer and the flow straightener are located 2D away from the outlet boundary. The upstream mixer is placed 4D away from the inlet boundary. The guide vanes are located in the elbow section for case 27. The four vanes are equally spaced according to Idelchik (1994) as shown in fig. 1(c). A square duct of equal diameter is placed near the inlet to study the branch effect for case 28. The branch is located 4.5D away from the inlet. 25% of air flow enters the branch inlet while 75% of air is supplied to the main inlet boundary for case 28. All simulation results are analyzed in terms of aerosol concentration (c), and cyclonic flow angle (β). Han et al. (2023) provided a detailed description of particle tracking modeling and considered turbulence models adopted in this study. The sampling grid influence is also included by comparing the 6" equal square section method (ACGIH, 1998) and the log-Techebycheff rule (ANSI/ASHRAE 111, 2008) with the full section values. All simulated cases are listed in table 1.

The grid density dependency is confirmed in terms of maximum velocity and maximum aerosol concentration at the outlet boundary. As shown in fig. 2, no significant change is detected at 326K cells, and the mesh with 326K cells is selected, which shows the 0.8% concentration and 1.2% velocity defference compared to the mesh with 487K cells. The mesh consists of prism and polyhedral shapes. There are five layers of prism mesh near the wall to capture the effect of boundary layer. The core of the duct is filled with polyhedral mesh, which significantly reduces the total number of cells compared to the tetrahedral mesh. However, the tetrahedral mesh is used to capture the louver-baffle mixing device geometry to avoid mesh quality degradation. The total number of cells in the louver-baffle case (Case 26) is 880K. The effect of the number of tracer particles on the aerosol concentration is also checked, and no difference is detected at 100,000 tracking particles. Therefore, a total 100,000 particles are tracked to estimate the aerosol concentration.

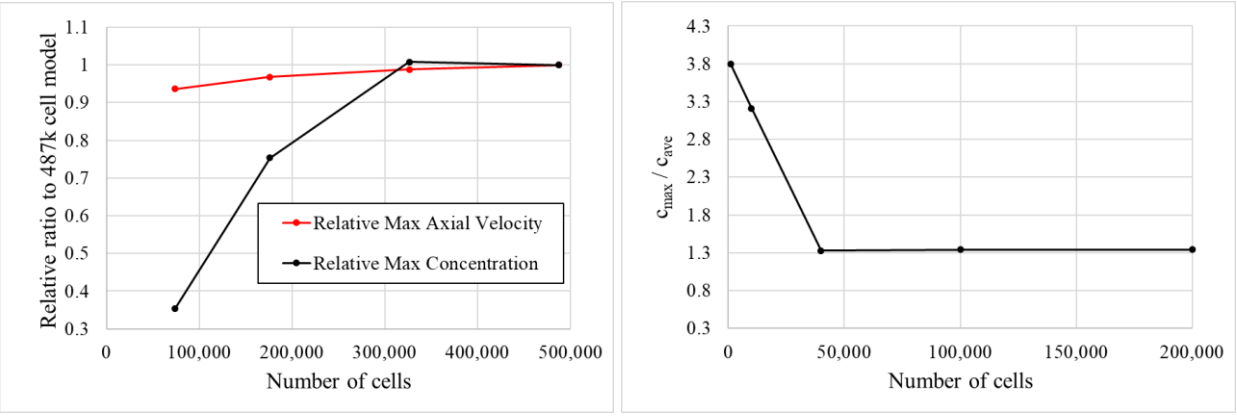

a) b)

Figure 2 (a) Grid dependency and (b) number of tracking particle dependency.

Table 1. Simulation Matrix

Case No.	n	v_d [fpm]	α [°]	d [μm]	m [μg/l]	vf	S_L	TM	TD	DRAG model	SHAPE
1	4	0	90	3	10	U	Inlet	S	DRW	SP	-
2	4	250	90	3	10	U	Inlet	S	DRW	SP	-
3	4	2500	90	3	10	U	Inlet	S	DRW	SP	-
4	4	2500	60	3	10	U	Inlet	S	DRW	SP	-
5	4	2500	120	3	10	U	Inlet	S	DRW	SP	-
6	4	0	90	3	100	U	Inlet	S	DRW	SP	-
7	4	0	90	1	10	U	Inlet	S	DRW	SP	-
8	4	0	90	3	10	F	Inlet	S	DRW	SP	-
9	4	0	90	3	10	T_{+Z}	Inlet	S	DRW	SP	-
10	4	0	90	3	10	T_{-Z}	Inlet	S	DRW	SP	-
11	1	0	90	3	10	U	Inlet	S	DRW	SP	-
12	1	0	90	3	10	U	UB	S	DRW	SP	-
13	1	0	90	3	10	U	45B	S	DRW	SP	-
14	1	0	90	3	10	U	$45S_{-Z}$	S	DRW	SP	-
15	1	0	90	3	10	U	$45S_{+Z}$	S	DRW	SP	-
16	1	0	90	3	10	U	R	S	DRW	SP	-
17	1	0	90	3	10	U	RUB	S	DRW	SP	-
18	4	0	90	3	10	U	R	S	DRW	SP	-
19	4	0	90	3	10	U	Inlet	RNG	DRW	SP	-
20	4	0	90	3	10	U	Inlet	R	DRW	SP	-
21	4	0	90	3	10	U	Inlet	RSM	DRW	SP	-
22	4	0	90	3	10	U	Inlet	S	NONE	SP	-
23	4	0	90	3	10	U	Inlet	S	DRW	NSP	-
24	4	0	90	3	10	U	Inlet	S	DRW	SC	-
25	4	0	90	3	10	U	Inlet	S	DRW	SP	ST
26	4	0	90	3	10	U	Inlet	S	DRW	SP	MD
27	4	0	90	3	10	U	Inlet	S	DRW	SP	G
28	4	0	90	3	10	U	Inlet	S	DRW	SP	B
29	4	0	90	3	10	U	Inlet	S	DRW	SP	MU

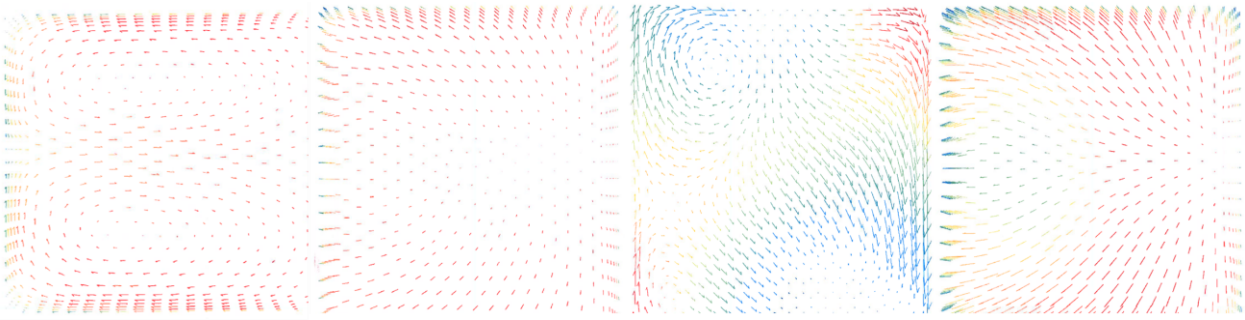

a) b) c) d)

Figure 3 Velocity vectors at the outlet for (a) Case 1, (b) Case 25, (c) Case 26, and (d) Case Case 27.

RESULTS

In this study, three key parameters are evaluated. The first term is the leakage rate, which represents the captured aerosols on the wall surface. The second term is the cyclonic flow angle (β), which is calculated from the axial,

rotational, and tangential velocities. One of the acceptance criteria of ANSI/HPS N13.1 (2021) is that the average composite angle based on all measurement grid points should be less than 20°. The last term is the ratio of the maximum (c_{max}) to the average (c_{ave}) aerosol concentration. ASME AG-1 (2019) requires that the aerosol concentrations over the entire sampling plane should not exceed ±20% of the average concentration. The simulation results as the sampling method are presented in Table 2. The all-node method uses all node data (1300 total) at the outlet. The equal-area (1998) method uses multiple identical rectangular cross sections. The total number of sampling points for the equal-area method is 400. ANSI 111 (2008) uses the log-Techbucheff rule, which provides 49 sampling points, which is advantageous from a measurement labor perspective.

The typical hydraulic behavior of a 90° elbow duct is presented in figures 3, 4, 5, and 6. The velocity vectors at the outlet boundary clearly show the presence of secondary flows caused by the sharp turn. A recirculation zone can be identified near the elbow exit in fig. 4. The aerosol trajectories closely match the streamlines. Due to the small inertia of the aerosol, its contribution to the air streamline distortion is limited.

The aerosol mixing behavior is unreasonable without considering the turbulent dispersion as shown in case 22 in figures 5 (b) and 6 (b). As shown in cases 1(S), 19 (RNG), 20 (R), and 21 (RSM), the influence of the turbulence model is more significant that that of other variables considered in this study. Hence, the turbulence model should be chosen carefully. The spherical (SP, Case 1), non-spherical (NSP, Case 23), and Stokes-Cunningham (SC, Case 24) drag laws have little effect on the three resulting parameters.

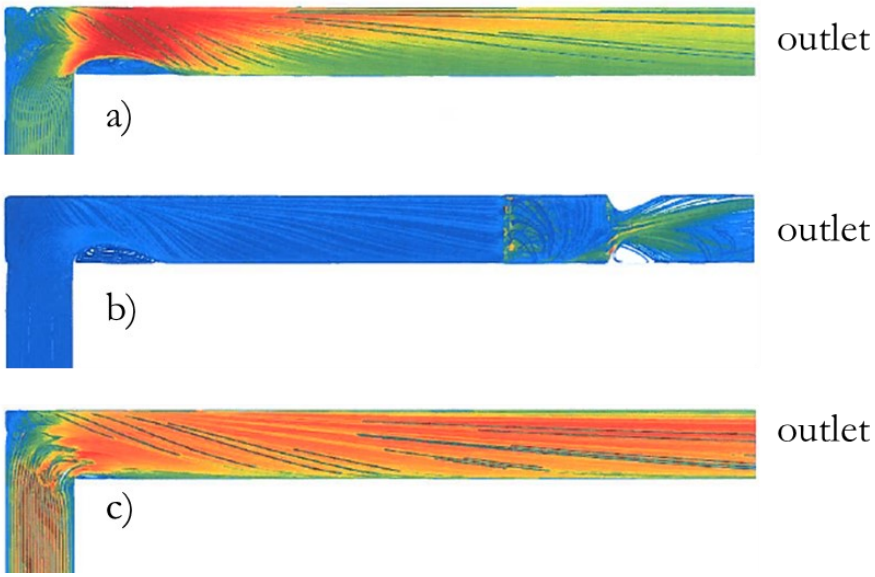

Figure 4 Streamlines for (a) Case 1, (b) Case 27, and (c) Case 26.

No distintive trend is detected as nozzle spray speed (Case 1, 2, 3) due to the small particle inertia. A wider nozzle cone angle is beneficial for improving mixing, as shown in Cases 1, 4, and 5. Cases 1, 8, 9, and 10 show that the velocity profile has strong influence. Case 1 has a uniform velocity profile (U). The fully developed velocity profile (F, Case 8) shows good mixing, whereas the triangular velocity profiles in Case 9 (T_{+z}: increasing velocity in the z-direction) and 10 (T_{-z}: decreasing velocity in the z-direction) show poor mixing. Interestingly, Case 9 has a cyclonic flow angle of 0. As arranged in Case 28, a duct can have multiple inlets, which affect the velocity profile. They generate unique velocity profile and mixing behavior, which is difficult to generalize in terms of aerosol concentration and swirl patterns. Increasing the aerosol amount (Case 6) helps mixing slightly. Reducing the aerosol diameter (Case 7) helps in achieving uniform mixing. ASME AG-1 (2019) states that 50% of the particles should be less than 0.7 μm

(3×10^{-5}") in diameter. Hence, the actual aerosol distribution is expected to be more uniform. Increasing the number of nozzles is recommended to achieve uniform aerosol concentration as shown in Case 11. Spraying the aerosol from wall should be avoided as in Cases 12 (UB, upward from bottom wall), 13 (45B, 45° inclined from bottom wall), 14 ($45S_{-Z}$, 45° inclined from -Z side wall), 15 ($45S_{+Z}$, 45° inclined from +Z side wall) and 17 (RUB, reverse spray upward from bottom wall). As fig. 5(d) illustrates, sprayed aerosol is pushed to the wall and most of the aerosol is trapped by the wall. It increases the leakage rate. Spraying the aerosol in the countercurrent direction (R, case 16 and 18) helps to reduce the non-uniformity of the aerosol concentration.

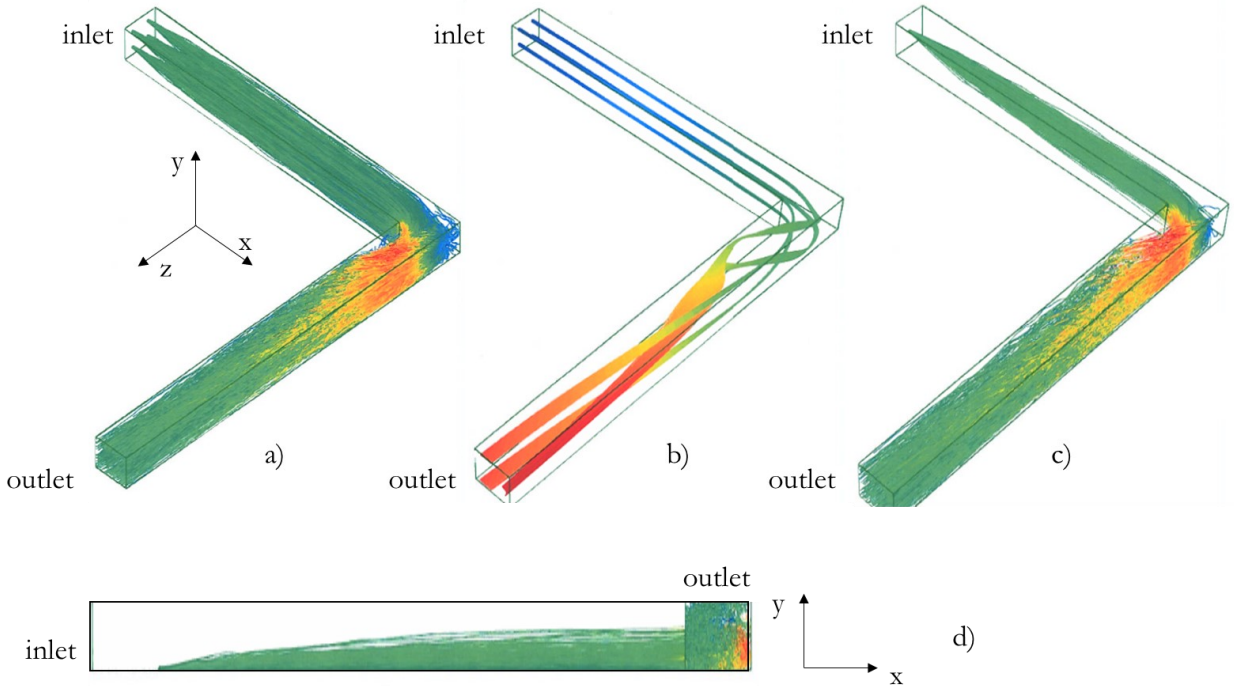

Figure 5 Aerosol trajectories for (a) Case 1, (b) Case 22, (c) Case 11, and (d) Case 12.

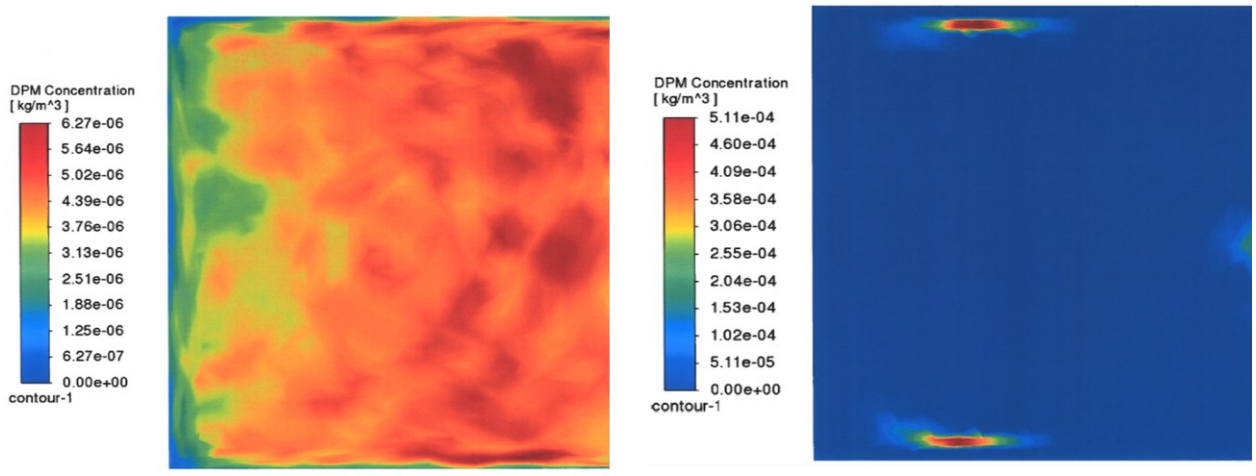

Figure 6 Aerosol concentration contours at the outlet for (a) Case 1 and (b) Case 22.

Except for the flow straightener (ST, Case 25), the downstream mixer (MD, Case 26), guidevanes (G, Case 27), upstream mixer (MU, Case 29) do not improve the mixing. The mixer worsens the swirl flow as shown in fig. 3 (c) and fig. 4 (b). Placing the mixer upstream (MU, Case 29) does not help reduce the cyclonic flow angle (β) and c_{max}/c_{ave} even though the actual standard deviation of aerosol concentration is reduced by 40% compared to Case 1. The guide vane (G, Case 27) reduces the pressure drop by up to 70%, whereas the flow straightener (ST, Case 25) and mixers (MD, Case 26) increase it by 22% and 5,100%, respectively. The introduction of these flow disturbance devices requires appropriate selection of fans and motors. It should also be noted that additionally efforts are required to inspect and clean the ducts for these flow devices.

Both the equal-area and Log-Tchebycheff methods capture flow rate (mean velocity) and cyclonic flow angle within 1% and 1°, respectively, in most cases except for the mixer (Cases 26 and 29). The Log-Tchebycheff method is known to perform poorly on velocity profiles with abrupt velocity changes, such as flow separation or recurculation, but the differences are not significant since the sampling plane is located well downstream of these flow disturbances. Overall, the equal-area results are similar to all-nodes method, while the Log-Tchebycheff method shows a lower c_{max}/c_{ave}.

ANSI/HPS N13.1 (2021) requires that velocity and aerosol concentration should not exceed 20% over the center region of the sampling plane that encompasses two-thirds of the area. Case 2 meets velocity fluctuation, aerosol concentration, and cyclonic flow angle requirements of ANSI/HPS N13.1 when the Log-Tchebycheff method is used.

Table 2. Simulation Results

Case No.	Leakage Rate [%]	All nodes		Equal area		Log-Tchebycheff	
		β [°]	c_{max}/c_{ave}	β [°]	c_{max}/c_{ave}	β [°]	c_{max}/c_{ave}
1	57	6	1.48	6	1.36	5	1.33
2	58	6	1.53	6	1.28	5	1.18
3	58	6	1.45	6	1.31	5	1.20
4	58	6	1.56	6	1.42	5	1.23
5	57	6	1.32	6	1.30	5	1.29
6	56	6	1.41	6	1.38	5	1.27
7	57	6	1.32	6	1.27	5	1.26
8	63	6	1.35	6	1.31	5	1.22
9	75	0	1.69	0	1.58	0	1.57
10	73	5	1.57	4	1.43	4	1.32
11	60	6	2.00	6	1.89	5	1.74
12	96	6	2.51	6	2.35	5	2.52
13	85	6	2.44	6	2.41	5	2.03
14	76	6	2.13	6	1.78	5	1.54
15	94	6	2.12	6	1.85	5	1.64
16	58	6	2.04	6	1.99	5	1.74
17	82	6	2.13	6	2.11	5	1.92
18	58	6	1.39	6	1.37	5	1.24
19	12	2	1.94	1	1.90	0	1.78
20	50	5	1.45	5	1.43	4	1.27
21	15	0	1.75	0	1.66	0	1.50
22	0	6	52.48	6	57.78	5	18.26
23	56	6	1.47	6	1.36	5	1.23
24	57	6	1.46	6	1.45	5	1.21
25	58	6	1.40	6	1.38	3	1.31
26	64	42	1.78	42	1.77	37	1.56
27	21	6	1.87	6	1.88	3	1.49
28	48	0	1.68	0	1.63	0	1.82
29	75	16	1.52	12	1.48	3	1.27

CONCLUSION

For a nuclear facility duct with 90° elbow, the aerosol concentration and air velocity patterns are analyzed with the assistance of CFD. ASME AG-1 standards are more stringent to meet because of strong recirculation and secondary flow, whereas ANSI/HPS N13.1 is easier to meet because it only uses central area samples for velocity and aerosol concentration fluctuations. Although velocity fluctuations and cyclonic flow angle variation easily meet ANSI/HPS N13.1 criteria, the aerosol concentration distribution parameter is still difficult to satisfy despite various attempts. A variety of modeling, operational, and geometrical parameters are evaluated to find a solution that can improve the aerosol distribution. Increasing the number of spray nozzles, widening the nozzle cone angle, spraying in the direction opposite to the air flow direction, and employing flow straighteners are found to improve the aerosol mixing uniformity and reduce swirl. Due to the unique velocity profile of each duct layout, a customized approach is required to improve mixing and minimize swirl flow. It is expected that the sampling plane and the spray nozzle can be arranged using CFD. However, the CFD model needs to be tuned with experimental data to select a turbulence model, adopt a drag model, and adjust turbulent dispersion parameters. It is also found that aerosol concentration profile varies depending on the sampling method.

REFERENCES

ASME. 2019. ASME AG-1-2019, Code on Nuclear Aur and Gas Treatment. New York: American Society of Mechanical Engineers.

ACGIH. 1998. Industrial Ventilation A Manual of Recommended Practice, 23rd Ed. Cincinnati: American Conference of Governmental Industrial Hygienists.

ANSI. 2021. ANSI/HPS N13.1-2021, Sampling and Monitoring Releases of Airborne Radioactive Substances from the Stacks and Ducts of Nuclear Facilities. Herndon: American National Standards Institute, Inc.

U.S. Government Publishing Office. 2024. Title 40 Protection of Environment Part 60. Washington DC: U.S. Government Publishing Office.

National Center for Biotechnology Information. 2024. PubChem Compound Summary for CID 8346, Dioctyl phthalate. https://pubchem.ncbi.nlm.nih.gov/compound/Dioctyl-phthalate. Accessed Nov. 5, 2024.

ISO. 2019. ISO 14644-3:2019, Cleanrooms and associated controlled environments – Part 3: Test methods. Geneva: International Organization for Standardization.

U.S. Department of Energy. 2022. DOE-HDBK-1169-2022, DOE Handbook: Handbook for use with DOE-STD-1269-2022, "Air cleaning systems in DOE nuclear facilities". Germantown: U.S. Department of Energy.

Gosman, A.D. and Loannides, E. 1983, Aspects of computer simulation of lqiud-fuelled combustors, *J. Energy* 7:482-490.

ASME. 2005. ASME MFC-3M-2004, Measurement of Fluid Flow in Pipes Using Orifice, Nozzle, and Venturi. New York: American Society of Mechanical Engineers.

Morsi, S.A. and Alexander, A.J. 1972. An Investigation of particle Trajectories in Two-Phase Flow Systems. *J. Fluid Mech.* 55:193-208.

Haider, A. and Levenspiel, O. 1989, Drag Coefficient and Terminal Velocity of Spherical and Nonspherical particles. *Powder Technology* 58:63-70.

Ounis, H., Ahmadi, G., and McLaughlin, J. B. 1991. Brownian Diffusion of Submicrometer Particles in the Viscous Sublayer. *J. Colloid and Inteface Science.* 143: 66-277.

Faison, T.K., Davis, J.C., Achenback, P.R., 1970. Performance of Louvered Devices as Air Mixers. Washington D.C.: U.S. Department of Commerce – National Bureau of Standards.

Idelchik, I.E. 1994. Handbook of Hydraulic Resistance, 3rd Ed. Boca Raton: CRC Press.

Han, K., Mistreanu, A., and D'Entremont, B., 2023. Numerical Analysis for Liquid Droplet and Thin Liquid Film Behavior in a Zig-Zag Drift Eliminator. *Int. J. Transport Phenomena*. 15: 181-192.

ASHRAE. 2008. *ANSI/ASHRAE Standard 111-2008*. Atlanta: ASHRAE.